

# Effects of Particle Size and Specific Surface Area of Porcelain Tile Polishing Waste on Self-compacting Mortars

Andrea Murillo Betioli, Morgana Fortunato, Ben-Hur Raíra Martins, Juliana Machado Casali, Janaíde Cavalcante Rocha, Giovana Collodetti

Federal Institute of Santa Catarina, Florianópolis, SC, Brazil.

---

**Abstract:** Current demands for shorter construction times and concerns about mitigating environmental impact are leading to the development of new technologies and encouraging waste recycling. The aim of this paper was to evaluate the influence of the addition of porcelain tile polishing residue (PPR) from two lots of the same factory in self-compacting mortar production. The water to cement ratio and the additive content were maintained the same. The results show that the PPR grain particle size and specific surface area affected the mortars' flowability and mechanical properties. Mortars with PPR0 (thicker particles than PPR1) presented increased compressive strength and a reduced air entrained, already from a 10% addition. In turn, the addition of PPR1 led to a decrease in the flowability of the mortars, maintaining a high rate of air entrained, which resulted in a lower gain of compressive strength. The results showed that the influence of the air-entrained rate on the compressive strength of the mortars prevailed over any possible improvements in particle packing and nucleation effects. Nonetheless, regardless of the amount and type of PPR used, the study shows the viability of using it to produce satisfactory self-compacting mortars.

**Key words:** self-compacting mortar; porcelain tile polishing waste; sustainability

---

## 1. Introduction

In the construction market, there is currently a growing acceleration of construction deadlines. There is an appreciation for cleaner, more industrialized construction sites. As a result, the development of new technologies is becoming increasingly common and necessary. One example is the use of self-compacting mortars for screeds. There are countless advantages of this mortar: reduced consumption of Portland cement and self-weight due to the small thickness; reduced labor and execution time; horizontality without the need for leveling; less chance of pathologies, among others (Martins, 2009).

Self-compacting mortar is a relatively new material in Brazil and began to be studied by construction companies and researchers in early 2008 (Martins, 2009). Some researchers indicate that, in order to obtain this mortar, high initial strength Portland cement (25% to 50% of the total mass), fine quartz sand (40% to 60%), 20% to 30% water in relation to the total dry mass of the mixture and the rest made up of additions and additives should be used (Nakakura; Bucher, 1997). However, the high consumption of Portland cement required for the flow of this mortar may lead to cracking of the underlying floor and have environmental impacts, as producing 1 ton of Portland cement emits 0.8 to 1 ton of CO<sub>2</sub>. It

---

Copyright © 2024 by author(s) and Frontier Scientific Research Publishing Inc.

This work is licensed under the Creative Commons Attribution International License (CC BY 4.0).

<http://creativecommons.org/licenses/by/4.0/>

---

should be noted that the cement industry is responsible for around 5% of all CO<sub>2</sub> emissions (World..., 2017).

In this way, replacing Portland cement with a mineral addition can prevent or reduce the shrinkage caused by Portland cement (Carvalho, 2015) and reduce the environmental impact it generates. This addition could be a finely particulate industrial by-product (steel, thermoelectric, food, aggregate production, etc.), an inert material or one with agglomerating characteristics. The most common are limestone filler, fly ash, metakaolin, blast furnace slag and active silica. The advantages of using additions to Portland cement-based materials can be:

- economic, by reducing the consumption of Portland cement (generally the most expensive component);
- technological, by improving fresh state properties, mechanical strength and durability; and
- environmental, by correctly disposing of or reusing industrial waste and reducing CO<sub>2</sub> emissions (released in the production of Portland cement) (Dal Molin, 2011).

Therefore, due to its environmental advantages, one of the proposed uses is porcelain tile polishing residue (PPR). During the polishing stage, around 100 g of PPR is generated per square meter of porcelain tile (Jacoby; Pelisser, 2015). The annual production of porcelain tiles is 152 million square meters, so it is estimated that 15.200 thousand tons of PPR are generated annually in Brazil, according to Anfacer (Associação..., 2019). Currently, very little of it is used in the ceramics industry itself, and its final disposal is usually in controlled landfills (Kummer et al., 2007). To dispose of this waste, PPR is classified as Class II A waste - Non-inert, i.e. a non-damaging waste that may have properties such as biodegradability, combustibility or solubility in water, according to the classification of solid waste (ABNT, 2004).

PPR is a finely particulate material derived from the surface wear of pieces, consisting mainly of the ceramic itself, with a small contribution of other compounds from the polishing and treatment of the waste (Andreola et al., 2010). Currently, PPR is not reused on a large scale, but what has been observed is an increase in research aimed at evaluating the potential for using this waste in cementitious materials, as in the case of coating mortar (Souza, 2013), concrete block (Steiner, 2011), concrete (Silva, 2005; Souza, 2007), self-compacting concrete (Matos et al., 2018) and as a supplementary cementitious material (Pelisser; Steiner; Bernardin, 2012; Steiner, 2014; Steiner; Bernardin; Pelisser, 2015; Jacoby; Pelisser, 2015).

Steiner, Bernardin and Pelisser (2015) evaluated PPR as a supplementary cementitious material and, replacing Portland cement with PPR, observed that the residue maintained the consistency of the mortars and showed a high level of pozzolanic activity, improving the efficiency index of Portland cement consumption (in kg/m<sup>3</sup>/MPa), reducing it by around 30%. The authors also found that the addition of PPR not only increased the time for shrinkage to begin, but also reduced autogenous shrinkage.

In concrete studies, Silva (2005) and Souza (2007) observed an increase in the compressive strength of concrete with the addition of PPR, as a result of the densification of the matrix by the filler effect and pozzolanic reactions. Jacoby and Pelisser (2011) observed that residues improved the workability and consistency characteristics of mortar. They also indicated that adding 20% PPR resulted in an average volcanic ash activity of 50%, as evidenced by the increase in compressive strength. Souza (2013) concluded that the incorporation of up to 20% PPR in coating mortar did not significantly alter the properties in the fresh and hardened states when compared to the reference mortar, a result of the PPR's filler effect, since it was analyzed at early ages.

In self-compacting concrete (SCC), studies carried out by Matos et al. (2018) showed that replacing Portland cement with up to 20% PPR obtained performances equivalent to those of the reference in the fresh state, up to 95% of its compressive strength at 91 days and up to 98% at 365 days, explained by the pozzolanic effect at advanced ages.

The chemical composition of PPR assessed by various authors cited by Matos (2019) shows, in general, that it is mostly composed of silica (58.90-68.97%) and alumina (15.49-21.04%). In addition, its particle size distribution is slightly finer than that of Portland cement, with a high specific surface area (around 10 times greater than that of Portland cement) (Pelisser; Steiner; Bernardin, 2012). In addition, several authors have proven the pozzolanic activity of PPR (Pelisser; Steiner; Bernardin, 2012; Steiner, 2014; Jacoby; Pelisser, 2015; Matos et al., 2018).

However, as noted by de Steiner (2014), there is variability in the results of chemical analysis and average diameters between different batches from the same company. Therefore, the particle size distribution and specific surface area of this waste should also be analyzed, as they can directly influence the rheology of cementitious materials, which is even more important for self-compacting materials.

Therefore, given the potential for reusing this waste, which is widely generated in the state of Santa Catarina and in Brazil, this study evaluated the effect of the particle size distribution and specific surface area of PPR on the properties of self-compacting mortar, with a view to reducing Portland cement consumption, as well as the technical feasibility of using it in these mortars.

## 2. Materials and Methods

The experimental program was divided into three parts. The first describes the materials used, the second, the production, and the third, the tests carried out on the self-compacting mortars.

### 2.1 Materials

The mortars were made with Portland cement composed of limestone filler (CPII F 32), fine aggregate (natural sand), limestone filler, dispersant additive (SP) and viscosity promoting additive (VMA). The sand used is a medium-fine sand, the grain size of which is shown in Figure 1 and the physical characterization of which is shown in Table 1, as well as the data for the limestone filler and Portland cement. Table 2 shows the characterization of the additives used.

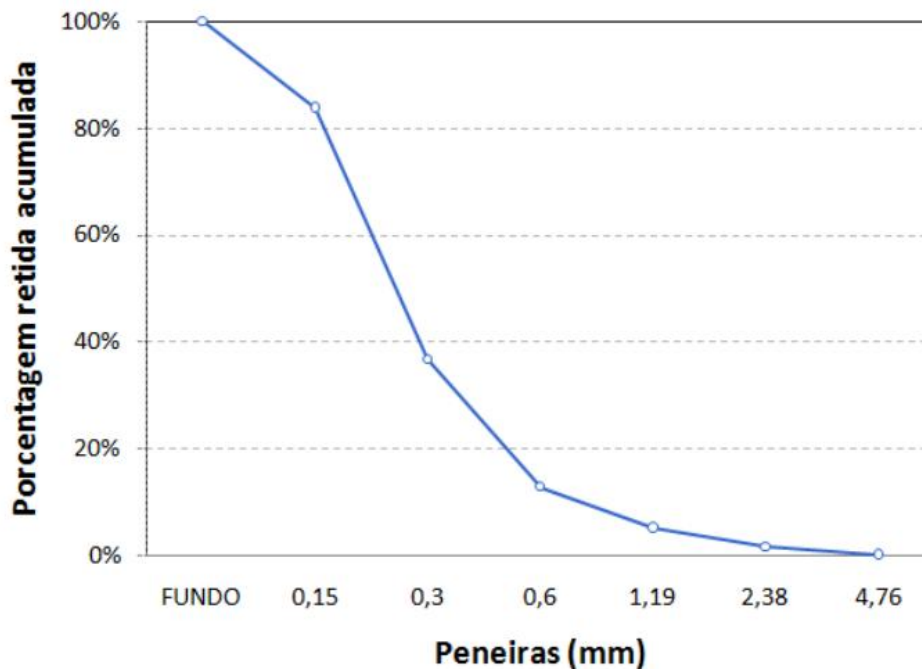


Figure 1. Particle size distribution of sand.

**Table 1.** Physical characterization of sand, limestone filler and Portland cement

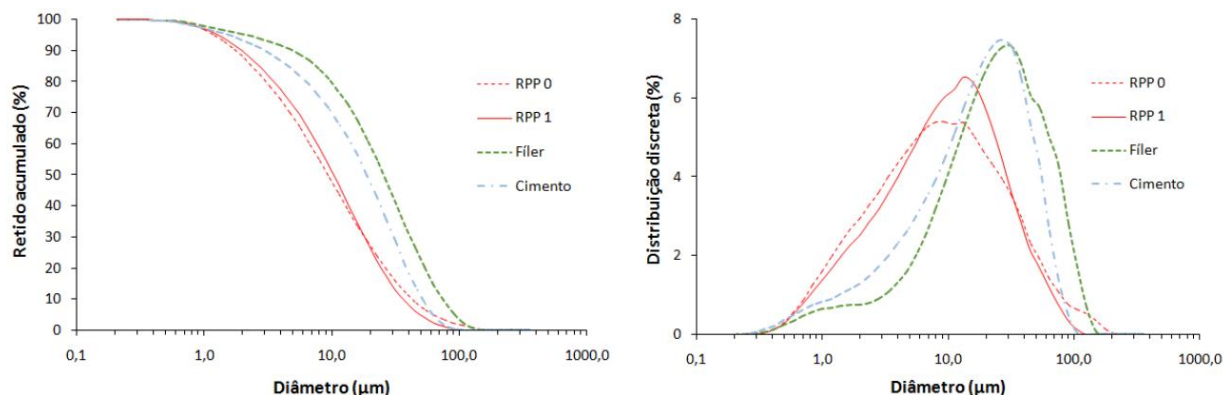
Material	Properties	Results
Natural sand	Specific mass ( $\text{g}/\text{cm}^3$ ) (ABNT, 2009)	2.60
	Maximum characteristic dimension (mm) (ABNT, 2003)	2.36
	Fineness modulus (ABNT, 2003)	1.49
Limestone filler	Specific mass ( $\text{g}/\text{cm}^3$ ) (ABNT, 2009)	2.70
Cement CP II F 32	Specific mass ( $\text{g}/\text{cm}^3$ ) (ABNT, 2017)	3.07
	Specific surface area ( $\text{m}^2/\text{g}$ )	0.98

**Table 2.** Characteristics of the additives used

Additives	Technical data			
	Characteristics	Unit	Value	Comments
SP	Density	$\text{g}/\text{cm}^3$	1.12	-
	Recommended dosage	%	0.2 - 5	Dosage in relation to the mass of cement
VMA	Density	$\text{g}/\text{cm}^3$	1.00	-
	Recommended dosage	%	0.1 - 1.5	Dosage in relation to cement mass

The PPR used in this research was collected at a company in the south of Santa Catarina. The PPR samples, called PPR0 and PPR1, were collected on different days over six months of production. Before the tests, they were dried in an oven at  $60 \pm 5^\circ\text{C}$  until their mass was constant and then crushed.

The particle size distributions were carried out using a Helos laser granulometer (Sympatec) with a detection range of  $0.1 \mu\text{m}$  to  $350 \mu\text{m}$ , as shown in Figure 2. It can be seen that PPR is a finer material than Portland cement and filler. The difference in particle sizes for the different PPRs collected from the same company is noteworthy, unlike what was observed by Steiner (2014). It can be seen that PPR0 has a greater number of coarser particles, which will be reflected in its specific surface area, described below.

**Figure 2.** Particle size curves obtained by laser granulometry of Portland cement CP II F, limestone filler and PPR0 and PPR1 waste.

The average diameter (D50) of the two PPR samples (PPR0 8.8  $\mu\text{m}$  and PPR1 7.9  $\mu\text{m}$ ) are lower than those of Portland cement (15.8  $\mu\text{m}$ ) and limestone filler (21.5  $\mu\text{m}$ ), and are within the limits presented by Pelisser, Steiner and Bernardin (2012) and Matos et al. (2018).

With regard to the material retained on the 45  $\mu\text{m}$  sieve, the results show possible pozzolanic activity in accordance with standards C618 (American..., 2012) and NBR 12653 (ABNT, 2015), when the material retained on the 45  $\mu\text{m}$  sieve must be  $\leq 34\%$  and  $\leq 20\%$  respectively, which is corroborated by the chemical analysis in Table 3 and confirmed by Matos et al. (2018), who used PPR from the same company in their research.

**Table 3.** Specific surface area and specific mass of the two PPR residues collected

Material	PPR0	PPR1
Specific surface area ( $\text{m}^2/\text{g}$ )	8.77	12.39
Specific mass ( $\text{g}/\text{cm}^3$ )	2.31	2.31

The specific surface area (SSA) was determined in Belsorp Max equipment, with the samples pre-treated at a temperature of 60°C and a pressure of  $10^{-2}$  kPa for 24 hours in Belprepvac-II equipment to remove moisture and other adsorbed gases. Table 3 shows the results of the specific surface area and specific mass (ABNT, 2009) of the two PPRs collected.

The chemical composition of the materials used was determined by X-ray fluorescence in Bruker's Sorter S1 industrial analysis equipment and is shown in Table 4. It can be seen that the composition of Portland cement CP II F 32 contains high levels of Ca and Si, followed by Al and Fe, and the limestone filler has a high calcium content, as expected. The PPR samples showed the highest concentrations of Si and Al, and low concentrations of Fe, K, and Ca — elements characteristic of ceramic materials, also observed by several authors cited by Matos (2019). The minimum and maximum values for these samples are 58.90% to 68.97% silica and 15.49% to 21.04% alumina. It can be seen that the PPRs in this study have higher silica values.

**Table 4.** XRF analysis of Portland cement CP II F, filler and PPR0 and PPR1 waste

	Cement	Filler	PPR0	PPR1
Oxide	%			
CaO	43.62	53.03	1.33	1.22
SiO <sub>2</sub>	33.24	4.66	74.00	72.64
Al <sub>2</sub> O <sub>3</sub>	6.94	-	16.34	17.27
Fe <sub>2</sub> O <sub>3</sub>	4.00	0.43	1.45	1.14
SO <sub>3</sub>	3.81	-	0.13	0.14
K <sub>2</sub> O	2.21	0.19	2.53	2.47
TiO <sub>2</sub>	0.70	0.05	0.30	0.23
SrO	0.22	0.28	-	-
MnO	0.10	0.01	-	-

	Cement	Filler	PPR0	PPR1
ZnO	0.06	-	0.30	-
ZrO <sub>2</sub>	-	-	0.14	0.43
Rb <sub>2</sub> O	-	-	0.17	0.19
MnO	-	-	0.05	0.04
CuO	-	0.02	0.05	0.04
Loss on ignition	5.00	41	3.15	3.92

As previously mentioned, the potential pozzolanic activity of PPR can be observed from the chemical analysis, since the sum of the percentages of SiO<sub>2</sub> + Al<sub>2</sub>O<sub>3</sub> + Fe<sub>2</sub>O<sub>3</sub> is approximately 91%, higher than the 70% recommended in the NBR 12653 (ABNT, 2015) and C 618 (American..., 2012) standards.

In order to evaluate the chemical components of the two residues studied, X-ray diffraction was carried out using a Shimadzu XRD 6000 diffractometer, a copper X-ray tube operating with Cu K $\alpha$  radiation ( $= 1.5418 \text{ \AA}$ ), a voltage of 30 kV and a current of 15 mA. The analysis was carried out from 10° to 80° (2 $\theta$ ) in a reading time of 2°/min.

Figures 3(a) and 3(b) show the diffractograms of the PPR0 and PPR1 samples and the main phases identified. The crystalline phases present in the materials are mainly related to the presence of quartz (SiO<sub>2</sub>) along with mullite (3Al<sub>2</sub>O<sub>3</sub>3SiO<sub>2</sub>) and albite (NaAlSi<sub>3</sub>O<sub>8</sub>) and silicon carbide (SiC). The phases identified are compatible with the results of the analysis of the total oxides, i.e. mostly made up of SiO<sub>2</sub>, Al<sub>2</sub>O<sub>3</sub>. These phases originate from the processing process, i.e. exposure to high firing temperatures and final finishing during polishing of the pieces. The presence of mullite is due to the transformation of kaolinite during the firing process. The other aluminosilicates are due to the reaction of kaolinite with other additives used in the processes. Silicon carbide is associated with the polishing process, as reported by Bernardin et al. (2006). A possible glassy phase is also assumed due to the formation of an amorphous halo (angle 2 $\theta$  from 15° to 32°), although this aspect was not explored in this article. According to Steiner (2014), this indicates that PPR is a potentially reactive material.

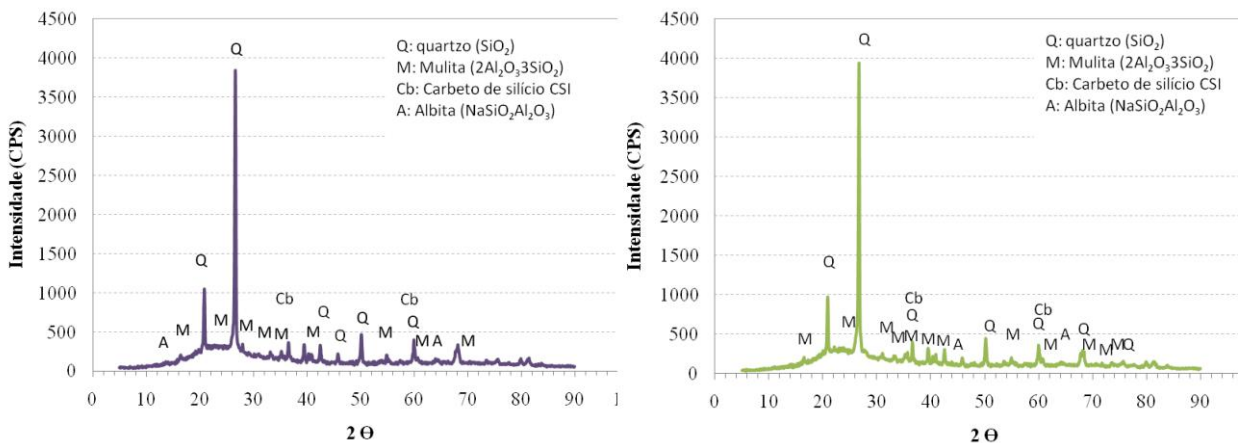


**Figure 3.** X-ray diffraction analysis of PPR0 and PPR1

In order to assess the surface and shape of the grains, images were taken of the PPR0 and PPR1 grains using a conventional scanning electron microscope (SEM) with a tungsten filament, JEOL JSM-6390LV (Figure 4). The dried samples were fixed with carbon tape to the base of the equipment support, coated with pulverized gold and kept in a vacuum desiccator until the date of analysis. In conjunction with the image analysis, it was possible to perform energy dispersive spectrometry (EDS), determining the approximate chemical composition of particles, regions or points of interest (Figure 5).

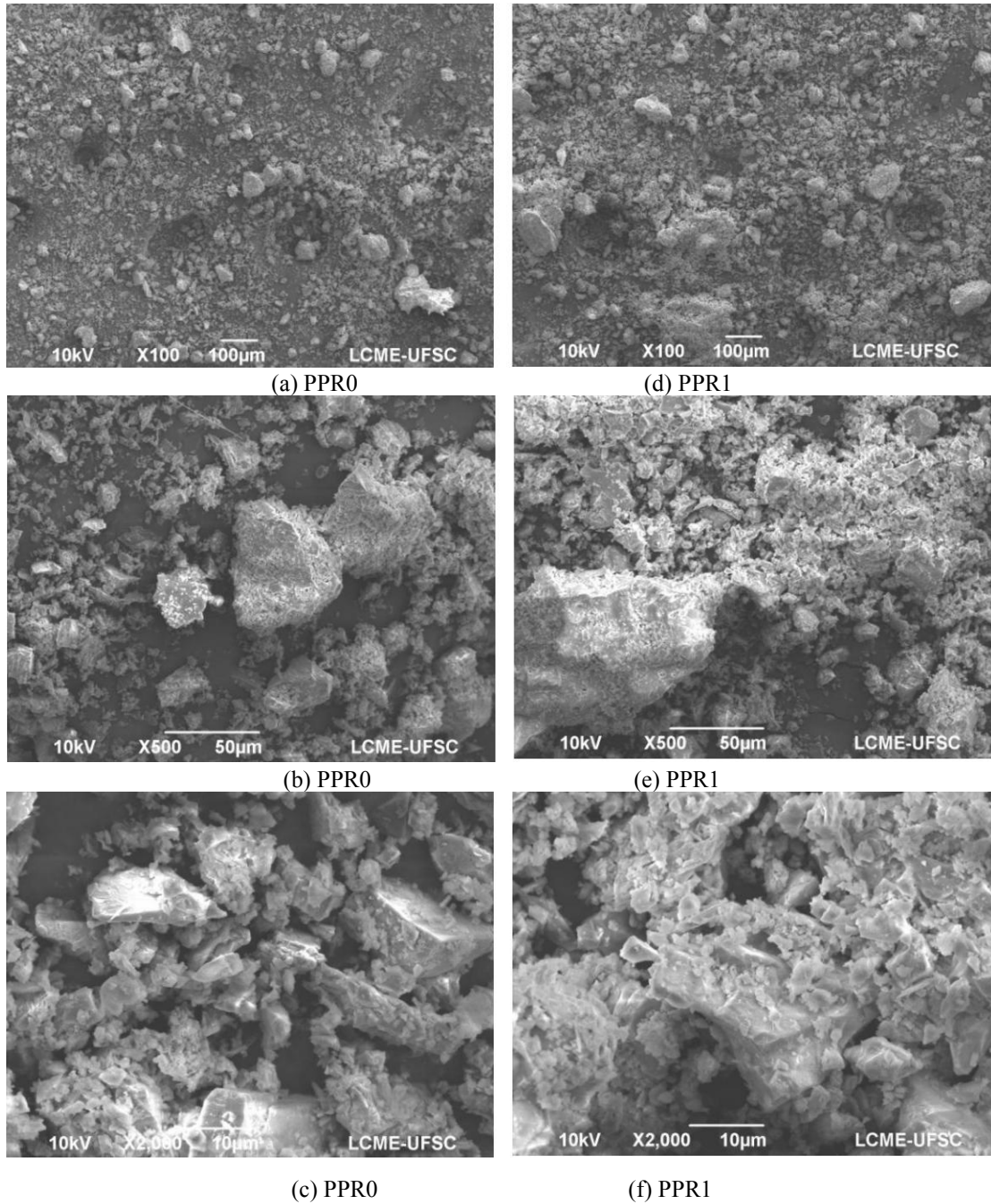


**Figure 4.** Micrographs of porcelain tile polishing residues PPR0 and PPR1.

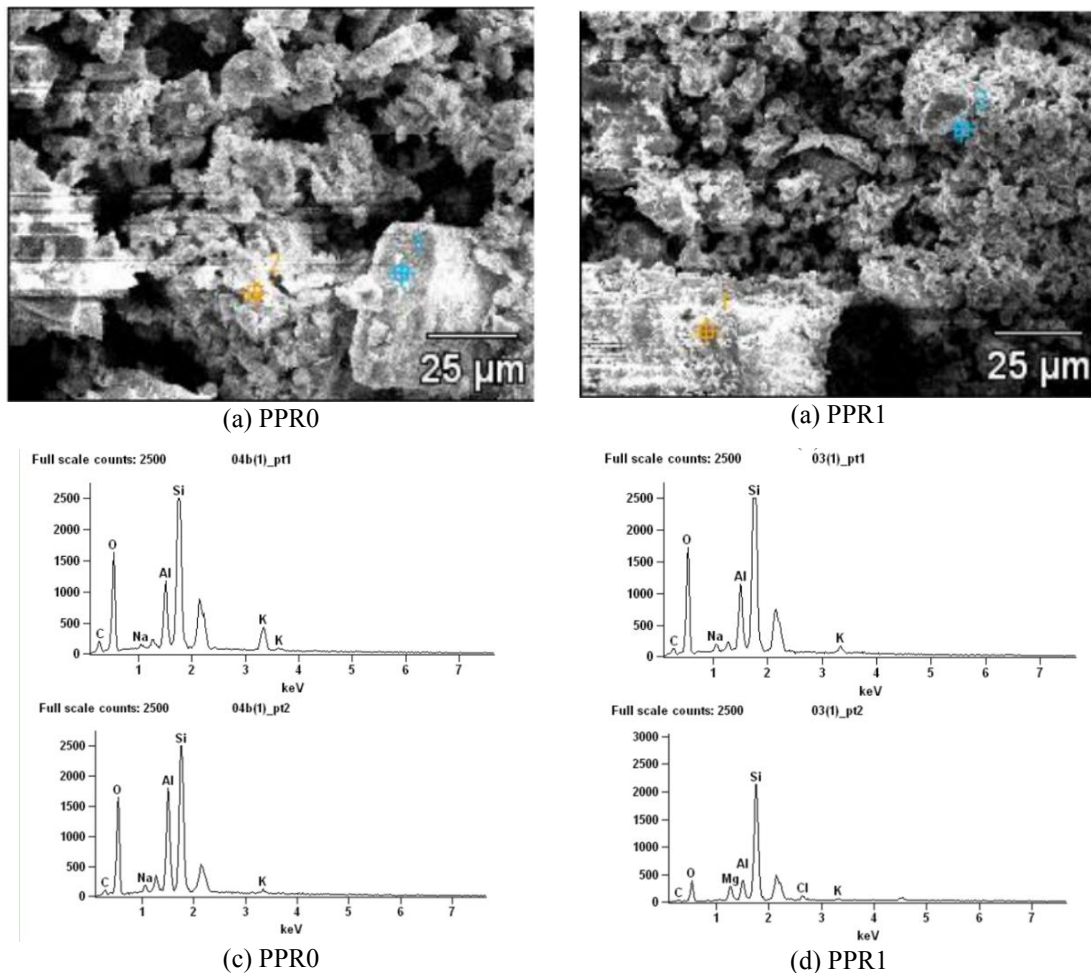


**Figure 5.** Micrographs of porcelain tile polishing residues PPR0 and PPR1.

Figure 4 shows the micrographs of the PPR grains at magnifications of 100x (a, d), 500x (b, e) and 2000x (c, f). It can be seen that the grains do not have a defined shape, being irregular and angular, which may influence the increase in water demand or the content of the dispersant additive.

Microanalysis using the EDS (X-ray scattering spectroscopy) probe was carried out on the approximations of the SEM images and aimed to verify the nature of the particles by analyzing the composition of the total oxides. In two morphologies, it was possible to identify the following elements detected at points (1) and (2) of the micrographs shown in Figure 5: predominantly silicon, aluminum and sodium and impurities such as potassium. The analyses are consistent with the phases identified in the diffractograms, indicating the presence of particles made up of albite, mullite and quartz.

## 2.2 Production of the self-compacting mortars

For the production of self-compacting mortars (SCC), a 1:3 mix (cement:sand, by mass) was used, with a constant water/cement ratio of 0.85 (by mass) and 50% limestone filler (in relation to the mass of Portland cement), based on the mix used by Martins et al. (2019). PPR0 and PPR1 waste was added at 10%, 20%, 30% and 50% in relation to the mass of Portland cement.

The SP and VMA additive contents (Table 5) were adjusted for the mortar made with PPR0 according to the spread values obtained (diameter greater than or equal to 220 mm), a parameter recommended by the European standard for AAA (European..., 2001). The additive concentrations were adjusted for the different PPR0 contents analyzed. These values were replicated for mortars with PPR1 in order to evaluate the effect of ASE and particle size.



**Table 5.** Quantity of SP and VMA additives used in relation to the mass of Portland cement

Additive	Reference	10% PPR	20% PPR	30% PPR	50% PPR
SP (%)	0.70	0.90	0.90	1.10	1.35
VMA (%)	0.70	0.70	0.70	0.70	0.70

As the two residues have the same specific mass (2.31 g/cm<sup>3</sup>), the volume added to the mortar was the same. The amount of each material used per cubic meter of mortar is shown in Table 6. It should be noted that even when PPR is used as an addition to, rather than a substitute for, Portland cement, as most researchers do, it can be seen that the consumption of Portland cement per cubic meter decreases as the amount of waste added increases.

**Table 6.** Actual consumption of AAA components in kilograms per cubic meter of fresh mortar

Mortars		Cement	Sand	Water	Filer	PPR	VMA	SP
Reference		373.34	1,120.04	317.34	186.67	0.00	2.61	2.61
10%	PPR0	371.09	1,113.28	315.42	185.55	37.11	2.60	3.33
20%		362.22	1,086.67	307.89	181.11	72.44	2.53	3.25
30%		360.27	1,080.81	306.23	180.13	108.08	2.52	3.96
50%		358.00	1,074.00	304.30	179.00	178.99	2.51	4.82
10%	PPR1	366.38	1,099.15	311.52	183.19	36.64	2.56	3.29
20%		350.63	1,051.91	298.04	175.32	70.13	2.45	3.15
30%		342.05	1,026.16	290.74	171.03	102.62	2.39	3.76
50%		339.56	1,018.68	288.62	169.78	169.78	2.38	4.58

The rheological, mobility and packing parameters of the compositions were estimated:

- volumetric surface area (VSA);
- specific surface area (SSA);
- porosity; separation distance between fine particles (IPS); and
- thickness of the paste layer between the aggregates (MPT).

The separation distance between the IPS was determined using Equation 1 (Oliveira et al., 2000):

$$IPS = \frac{2}{VSA} X \left[ \frac{1}{V_s} - \left( \frac{1}{1 - Pof} \right) \right] \quad \text{Eq. 1}$$

Where:

*VSA* is the volumetric surface area (product of the specific surface area and the actual density of the powder);

*V<sub>s</sub>* is the volume fraction of solids; and

*Pof* is the theoretical porosity of the system, when all the particles of the matrix are in contact in the condition of maximum packing, estimated according to the method of Westman and Hugill (Westman, Hugill, 1930; Oliveira et al., 2000).

According to Maciel et al. (2018), the original *IPS* equation can be used to determine the thickness of the paste layer that keeps the *MPTs* away, modifying the parameters  $VSA_g$  (volumetric surface area of the coarse fraction),  $Pof_g$  (theoretical porosity of the coarse particle distribution, Westman and Hugill method) and  $Vs_g$  (volumetric concentration of the coarse particles), as shown in Equation 2.

$$MPT = \frac{2}{VSA_g} \times \left[ \frac{1}{Vs_g} - \left( \frac{1}{1 - Pof_g} \right) \right] \quad \text{Eq. 2}$$

The mortar mixing process was carried out in a planetary mortar mixer, in the following sequence: mix the dry materials for 60 seconds, then add 50% of the water and mix for another 60 seconds, then add the rest of the water and mix for 60 seconds. After the initial procedure, with the mortar turned off, the dispersant additive (SP) was added and the mortar turned on for another 60 seconds. Finally, the viscosity promoting additive was added and mixed for 120 seconds.

### 2.3 Fresh and hardened tests

The following properties were determined in the fresh state:

- segregation and exudation (edge appearance analysis);
- fluidity and workability through the spread test on the table, based on the minicone, according to NBR 13276 (ABNT, 2016), but without the application of blows; and
- mass density and incorporated air content in accordance with NBR 13280 (ABNT, 2005a).

In the hardened state, apparent mass density, according to NBR 13280 (ABNT, 2005a); and compressive strength and tensile strength in bending, according to NBR 13279 (ABNT, 2005b) at 28 days, were evaluated. The results were evaluated according to the parameters established by the European standard (European..., 2001), which suggests values  $\geq 5$  MPa for tensile strength in bending, and values  $\geq 20$  MPa for compressive strength. The Duncan test was used for statistical analysis of the results.

After 48 h in the mold, the specimens were kept for 5 days in an environment with  $95 \pm 5\%$  humidity, and 21 days in  $65 \pm 5\%$ , with a temperature of  $23 \pm 2^\circ\text{C}$ , as recommended by EN 13892-1 (British..., 2002).

The efficiency of mortars using PPR was evaluated through the Binding Intensity Index (IL) (Damineli, 2013). The value is obtained by the ratio between Portland cement consumption of the mortar in kilograms per cubic meter and the value obtained of compressive strength in the hardened state, in Megapascal (Equation 3). This value allows a comparison of the different mortars evaluated. The higher its value, the greater the amount of Portland cement used for the same function. In this case, the compressive strength at 28 days is higher, resulting in lower ecological efficiency of the mixture. The efficiency percentage was calculated with Equation 4.

$$IL = \frac{\text{Cement consumption (kg/m}^3\text{)}}{\text{Compressive strength (MPa)}} \quad \text{Eq. 3}$$

$$\%Efficiency = \frac{IL_{reference} - IL_{firedmortar}}{IL_{reference}} * 100 \quad \text{Eq. 4}$$

Where:

$IL$  is the index of binder intensity;

$IL_{reference}$  is the binder intensity of the reference mortar; and

$IL_{firedmortar}$  is the binder intensity of the mortar with PPR.

### 3. Results and Discussions

The calculated rheological parameters, mobility and packaging of the compositions, are shown in Table 7. It is noteworthy that, to calculate the thickness value of the slurry layer that separates the aggregates (MPT), the air content was not taken into account because this is a function of the mixing condition. If the air content was the same, the composition with PPR0 would require more paste to separate the grains, because, according to Romano et al. (2016), when the paste content is sufficient to exceed the porosity of the system and cover the surface of the particles, the system can be expected to flow.

**Table 7.** Solid particle mobility and packaging parameters of reference compositions and using PPR0 and PPR1

Waste	Mortars	ASV (m <sup>2</sup> /cm <sup>3</sup> )	ASE (m <sup>2</sup> /g)	Porosity (%)	IPS (μm)	MPT (μm)
-	Reference	1.32	0.48	10.52	1.114	2.229
PPR0	10%	1.82	0.66	9.74	0.655	2.322
	20%	2.29	0.83	8.99	0.464	2.413
	30%	2.73	1.00	8.25	0.359	2.499
	50%	3.54	1.31	6.76	0.248	2.675
PPR1	10%	2.03	0.74	9.71	0.559	2.326
	20%	2.71	0.99	8.92	0.372	2.42
	30%	3.35	1.23	8.15	0.278	2.51
	50%	4.53	1.67	6.58	0.185	2.694










It is noted that compositions with the addition of porcelain polishing residue PPR1 present higher values of ASV and ASE, and lower separation distance between the IPS due to the larger specific surface area of the grain and the finer granulometry. This difference can impact, for example, the demand for water or additive, since the increase in the specific area of the systems, for example, can result in increased water demand for kneading and maintenance of the desired consistency. The theoretical packaging porosity indicates the volume of microstructural voids resulting from the combination of raw materials. It is observed that the addition of PPR1 reduces the porosity of the system.

The values obtained for spreading diameter of self-compacting mortars are shown in Table 8, together with mass density. The photographic records for the analysis of border uniformity are presented in Table 9.

**Table 8.** Spread values in minicone test and fresh mass density of reference mortars using PPR0 and PPR1

Mortars	REF	10%		20% PPR		30% PPR		50% PPR	
		PPR0	PPR1	PPR0	PPR1	PPR0	PPR1	PPR0	PPR1
Minicone (mm)	279	327.5	322.5	302.5	237.0	325.0	286.5	360.0	207.5
Mass density (g/cm <sup>3</sup> )	2.00	2.02	2.02	2.02	1.95	2.04	1.94	2.10	1.99

**Table 9.** Scattering images of self-compacting mortars reference and using PPR0 and PPR1

Reference	10%	20%	30%	50%
	PPR0			
				
	PPR1			
				

It is possible to note that, except for mortar with 50% PPR1 (PPR of larger specific surface area), all mortars analyzed obtained scattering values within the standard (diameter  $\geq 220$  mm). This occurred due to the adjustment in the amount of SP additive (Table 5) according to the amount of PPR0 used in the mixture. The increase in SP additive content was necessary because the higher the amount of fine in the mixture, the higher the viscosity of the mortar and, consequently, the lower its fluidity (Figure 6). The use of fine with a large specific surface area results in greater water adsorption, reducing the fluidity of the mixture (Carvalho, 2015), and the particle size distribution of the PPR is thinner than that of Portland cement (Peliser; Steiner; Bernardin, 2012). In this case, the high specific surface area of the residues (about 10 times larger than Portland cement, Tables 1 and 2) reduced the free water of the mixture, making the mortar more viscous. Matos et al. (2018) also observed this fact in self compacting concrete.

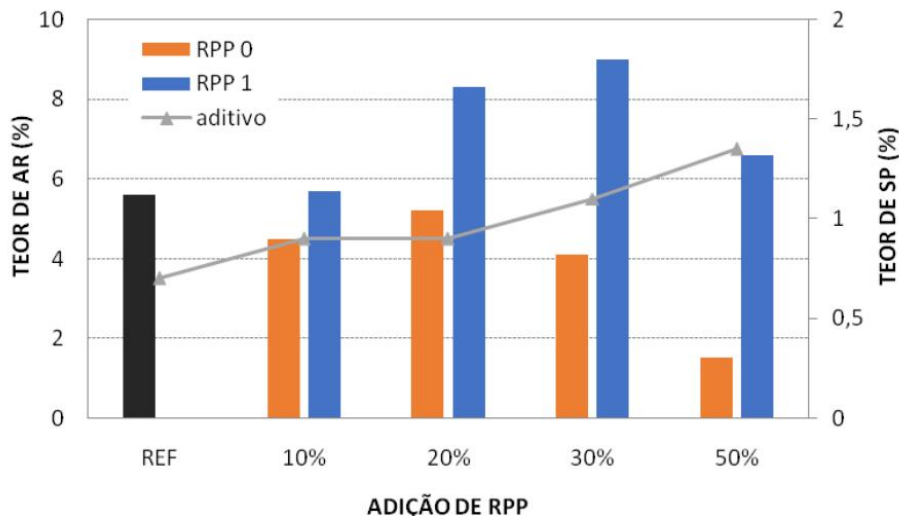


**Figure 6.** Incorporation content and additive content SP in reference mortars and using PPR0 and PPR1.

All mortars presented uniform edges without traces of segregation or exudation, but keeping the additive content constant showed that PPR0, because it has a smaller specific surface area and thicker particles, requires a lower additive content. This effect can be verified in the images in Table 9, in which AAA with PPR0 present more uniform scattering and better edge appearance than those with PPR1.

Comparing the effects of PPR, it is worth noting that compared to PPR0, PPR1 is thinner, has a larger specific surface area, and requires higher additive content under the same fluidity. Matos et al. (2018) observed this fact, where it is necessary to increase the additive content when replacing Portland cement with PPR to maintain fluidity. Thus, for this study, in which the SP additive content was fixed for the same PPR addition content, the mortar with PPR1 showed lower fluidity (Table 8).

Figure 6 shows the air content incorporated in self-compacting mortars with different percentages of addition of PPR0 and PPR1, and the content of SP additive used. According to Mattana and Costa (2010), the effect of the dispersing additive can cause greater incorporation of air. There is an increase in the incorporated air content with an increase of the additive SP, up to a limit of addition content, for PPR0 up to 20% and for PPR1 up to 30%. After this limit, there was a decrease in the incorporated air content.

It is also observed in Figure 6 that the lower air content incorporated in mortars with PPR0 can be explained by the lower viscosity of the paste, which reduces the stability of air bubbles, accelerating coalescence and elimination of them (Romano et al., 2012). After adding PPR1, the opposite situation was observed (Figure 6), where the lower flowability and greater cohesion of the mortar maintained the stability of the trapped air during the mixing process. This result already demonstrates that the variability of granulometry and specific surface area of PPR produced by the same plant can alter the consumption of superplasticizer additive for certain fluidity and, even more importantly, influence the incorporated air content, which may affect the performance in the hardened state, as shown in Figures 7 and 9.

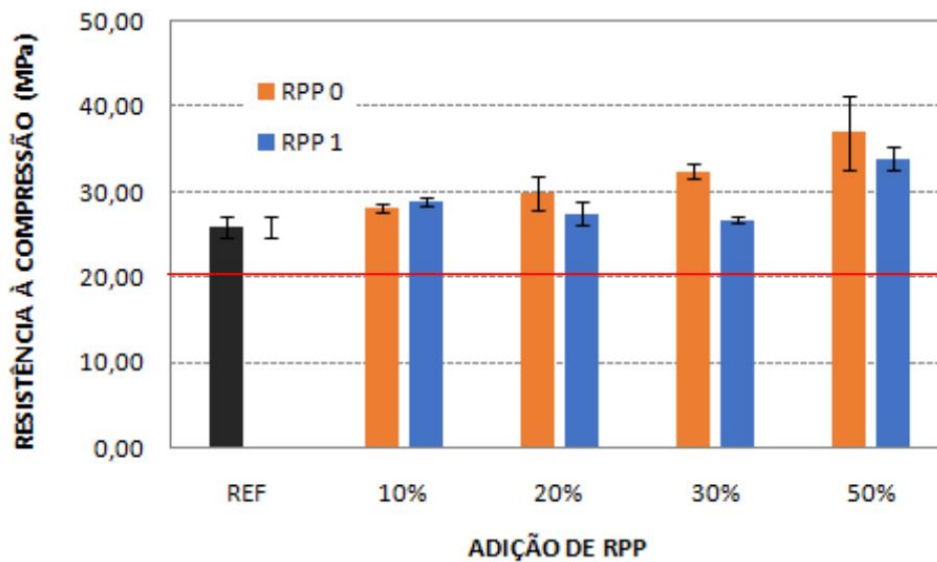


**Figure 7.** Compressive strength of reference mortars and using PPR0 and PPR1.

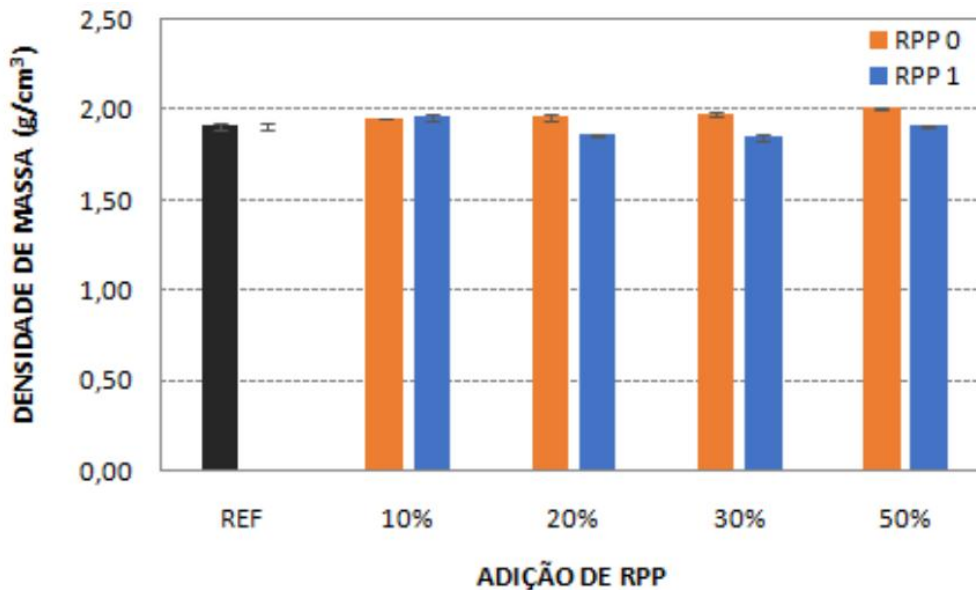


Figure 8. Mass density in the hardened state of reference mortars and using PPR0 and PPR1.

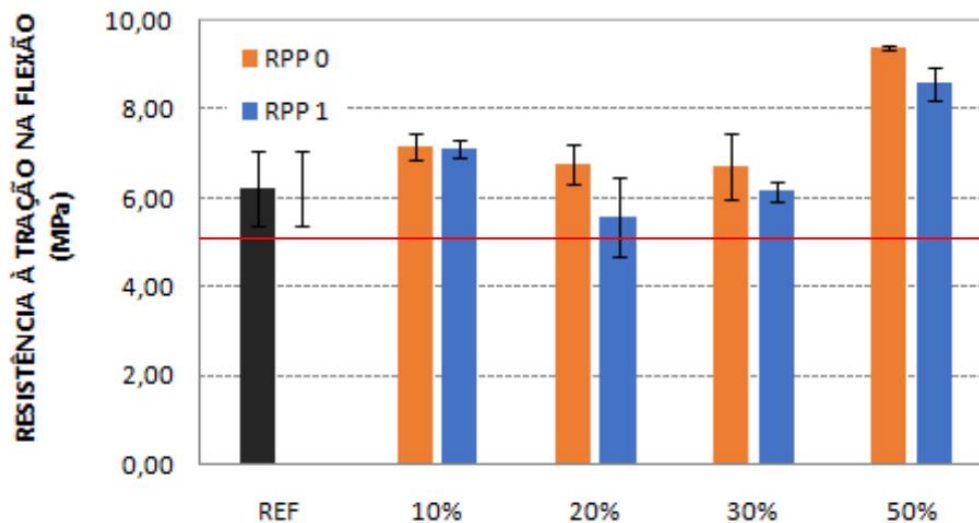


Figure 9. Tensile strength in bending of reference mortars and using PPR0 and PPR1.

It is observed in Figure 7 that the compressive strength values had values higher than the minimum required by the standard (20 MPa - indicated with a full line in Figure 7) for all mortars tested. It is also noted that the addition of PPR0 increased the compressive strength with the increase in the PPR content added. The addition of 20% and 30% of PPR1 did not alter the compressive strength due to the incorporated air content and, only with the use of 50% of this residue, it was observed an increase of 40% of the strength in relation to the reference.

The increase in compressive strength with the use of PPR was also observed by Pelisser, Steiner and Bernardin (2012). According to the authors, the isothermal calorimetry showed an increase in the heat released with the increase in the PPR content, indicating potentiation in the hydration kinetics by the availability of nucleation points for the formation of C-S-H gels. Furthermore, the authors attributed this increase to the pozzolanic activity of the residue, since they made an evaluation over time (up to 56 days) and to the filler effect, due to the reduction in porosity and permeability of the matrix. Pozzolanic activity was also proven by Steiner (2014), Jacoby and Pelisser (2015) and Matos et al. (2018).

The analysis in this research was performed at 28 days. Thus, possibly, this increase can be attributed mainly to the improvement in the granulometric packaging of the mixture by decreasing the volume of voids, as mentioned by Fiorentin (2011), as shown in the reduction of the porosity of the skeleton in Table 7 for the two PPR residues used.

It is known that the main factor governing the mechanical strength of cement-based materials is the water/cement ratio. However, according to Matos (2019), the use of inert mineral additions (widely used in self-compacting concretes) can improve the packaging of the material, reducing porosity and, consequently, increasing its mechanical strength. Uysal and Yilmaz (2011) reiterate that the best packaging promoted by additions forms denser matrices, in addition to providing better dispersion of cement grains and formation of nucleation points for C-S-H gels.

Regarding the different PPR evaluated, as the water/cement ratio was kept constant, the higher content of embedded air trapped in mortars with PPR1 may have influenced for a lower strength gain, because, according to Torres, Romano and Pileggi (2017), porosity may represent critical defects that decrease mechanical strength, as can be seen in the values of mass density in the hardened state.

Despite the larger specific surface area of PPR1 and the lower theoretical porosity of the system, (Table 7), the air content in self-compacting mortars with this residue was higher (Figure 6), consequently lower apparent mass density (Figure 8), possibly influencing a lower gain in compressive strength (Table 10) in relation to self-compacting mortars with the addition of PPR0, as already mentioned.

**Table 10.** Compression strength and gain in relation to the mortar reference

REF		Compressive strength (MPa)	Gain on resistance %
		25.8	
10%	PPR0	28.1	8.9%
	PPR1	28.9	11.8%
20%	PPR0	29.9	15.7%
	PPR1	27.5	6.3%
30%	PPR0	32.4	25.6%
	PPR1	26.8	3.6%
50%	PPR0	38.6	49.6%
	PPR1	33.9	31.4%

The flexural tensile strength values showed great variability (Figure 9), and it was only possible to observe a significant increase with the use of 50% PPR for both types evaluated; again, the effect of air content was higher for mortars with PPR1.

It is observed that the values of tensile strength in bending, as well as the values of compressive strength, had values higher than the minimum required by the standard (5 MPa) for all mortars tested.

Tables 11 and 12 show the results of the efficiency index for the mortars studied. As can be observed, as the use of PPR increases, IL decreases and mortar efficiency increases, thus enabling reduction of Portland cement consumption. This behavior was more evident for PPR0, despite smaller specific area and thicker granulometry, because its use resulted in greater gains in resistance, as previously commented and presented in Table 10.

**Table 11.** Results of the efficiency index of each mortar studied with PPR0

	REF	10% PPR0	20% PPR0	30% PPR0	50% PPR0
IL (kg/m <sup>3</sup> . MPa-1)	14.47	13.20	12.13	11.11	9.27
% Efficiency	0.00%	8.77%	16.16%	23.20%	35.89%
Cement reduction (kg/m <sup>3</sup> )	0.00	2.25	11.12	13.08	15.35

**Table 12.** Results of the efficiency index of each mortar studied with PPR1

	REF	10% PPR1	20% PPR1	30% PPR1	50% PPR1
IL (kg/m <sup>3</sup> . MPa-1)	14.47	12.70	12.78	12.79	10.01
% Efficiency	0.00%	12.24%	11.69%	11.60%	30.77%
Cement reduction (kg/m <sup>3</sup> )	0.00	6.97	22.71	31.29	33.79

Thus, an improvement in the properties of the hardened state of self-compacting mortars using PPR was demonstrated, and an efficiency index of 35.89% was verified for the use of 50% of PPR0 (Table 11), thus enabling an even greater reduction in Portland cement consumption per cubic meter for the same strength.

#### 4. Conclusions

The purpose of this research was to evaluate the effect of the specific surface area and granulometry of porcelain polishing residues in the production of self-compacting mortars. The samples, different PPR residues, showed that, despite the similar chemical composition, the differences in particle size composition and specific surface area altered the performance of the properties of the self-compacting mortar in the fresh and hardened state.

Regardless of the PPR used, the results were satisfactory when added to self-compacting mortars. Despite the need to adjust the amount of superplasticizer additive, according to the increase in the addition of PPR, the mortars showed an increase or did not influence the strength, and one resulted in a reduction in Portland cement consumption per cubic meter. These results can be explained by the filler effect of adding the fine, resulting in improved system packaging.

Although the water/cement ratio and additive contents were kept constant, adjusted for mortars with PPR0, the addition of PPR0 residue (smaller specific surface area and thicker particles) resulted in lower incorporated air content, and the increase in strength occurred already from 10% of addition. As for PPR1 (larger specific surface area and thinner particles), the compressive strength increased with additions above 30%. Higher strengths were expected with the addition of PPR1, because the theoretical porosity of this composition is lower, which would result in better packaging, but this did not occur possibly due to the higher viscosity and cohesion of the mortar, which eventually stabilized the air in the mixture, presenting higher content of air incorporation.

Thus, regardless of the content and type of PPR used, since the chemical composition is similar and there is only difference in particle size composition and specific surface area of PPR grains, the results were satisfactory when the residue was added to self-compacting mortars. Therefore, the use of these residues is feasible as fines in self-compacting mortars, which allows the use of a residue resulting from a production process.



## Acknowledgments

The authors would like to thank CNPq, the Federal Institute of Santa Catarina (IFSC) - Florianópolis Campus and the National Institute for Advanced Eco-efficient Cement Technologies (FAPESP INCT 465593/2014-3). They would also like to thank Eliane Revestimentos, MC-Bauchemie and Itambé for donating the materials used in this research.

## Declaration

Efeito da composição granulométrica e da área superficial específica de resíduos de polimento de porcelanato em argamassas autoadensáveis was originally published in *Revista Ambiente Construído*. With the author's consent, the English version Effects of Particle Size and Specific Surface Area of Porcelain Tile Polishing Waste on Self-compacting Mortars has been published in *Journal of Building Technology*.

## Conflicts of Interest

The author declares no conflicts of interest regarding the publication of this paper.

## References

- [1] Westman, A. E. R.; Hugill, H. R. The packing of particles. *Journal of American Ceramic Society*, v. 13, n. 10, p. 767-779, 1930.
- [2] American Society for Testing and Materials. C618-05: Standard Specification for Coal Flyash and Rawor Calcined Natural Pozzolan For Use In Concrete. Philadelphia, 2012.
- [3] Andreola, F. et al. New blended cement from polishing and glazing ceramic sludge. *International Journal of Applied Ceramic Technology*, v. 7, n. 4, p. 546-555, 2010.
- [4] Associação Brasileira De Normas Técnicas. NBR 10004: resíduos sólidos: classificação. Rio de Janeiro, 2004.
- [5] Associação Brasileira De Normas Técnicas. NBR 12653: materiais pozolânicos: requisitos. Rio de Janeiro, 2014. Versão corrigida: 2015.
- [6] Associação Brasileira De Normas Técnicas. NBR 13276: argamassa para assentamento e revestimento de paredes e tetos: determinação do índice de consistência. Rio de Janeiro, 2016.
- [7] Associação Brasileira De Normas Técnicas. NBR 13279: argamassa para assentamento e revestimento de paredes e tetos: determinação da resistência à tração na flexão e à compressão. Rio de Janeiro, 2005b.
- [8] Associação Brasileira De Normas Técnicas. NBR 13280: argamassa para assentamento e revestimento de paredes e tetos: determinação da densidade de massa aparente no estado endurecido. Rio de Janeiro, 2005a.
- [9] Associação Brasileira De Normas Técnicas. NBR 16605: cimento Portland e outros materiais em pó: determinação da massa específica. Rio de Janeiro, 2017.
- [10] Associação Brasileira De Normas Técnicas. NBR NM 248: agregados: determinação da composição granulométrica. Rio de Janeiro, 2003.
- [11] Associação Brasileira De Normas Técnicas. NBR NM 52: agregado miúdo: determinação de massa específica e massa específica aparente. Rio de Janeiro, 2009.
- [12] Associação Nacional Dos Fabricantes De Cerâmica Para Revestimentos, Louças Sanitárias e Congêneres. Números do setor. Disponível em: <https://www.anfacer.org.br/> Acesso em: 20 set. 2019.
- [13] Bernardin, A. M. et al Reaproveitamento de resíduos de polimento e de esmaltação para obtenção de cerâmica celular. *Cerâmica Industrial*, v. 11, p. 41-34, 2006.
- [14] British-Adopted European Standard. BS EN 13892-1: Method of Test for Screed Materials: Sampling, Making and Curing Specimens For Test. London, 2002.

- [15] Carvalho, H. D. S. Análise de retração por secagem em argamassas autonivelantes utilizando adições minerais como substitutos parciais do cimento Portland Florianópolis, 2015. 138 f. Dissertação (Mestrado em Engenharia Civil) - Curso de Engenharia Civil, Universidade Federal de Santa Catarina, Florianópolis, 2015.
- [16] Dal Molin, D. C. C. Adições minerais. In: ISAIA, G.C. Concreto: ciência e tecnologia. São Paulo: Ibracon, 2011.
- [17] Damineli, B. L. Conceitos para formulação de concretos com baixo consumo de ligantes: controle reológico, empacotamento e dispersão de partículas. 2013. Tese (Doutorado em Engenharia de Construção Civil e Urbana) - Escola Politécnica, Universidade de São Paulo, São Paulo, 2013.
- [18] European Federation for Specialist Construction Chemicals and Concrete Systems. Specification for Synthetic Resin and Polymer-Modified Cementitious Floorings As Wearing Surfaces for Industrial and Commercial Use. London, 2001.
- [19] Fiorentin, T. R. Influência do aditivo modificador de viscosidade e do filler calcário no comportamento de pastas e argamassas de concreto autoadensável Pato Branco, 2011. 68 f. Trabalho de Conclusão de Curso (Bacharelado em Engenharia Civil) - Universidade Tecnológica Federal do Paraná, Pato Branco, 2011.
- [20] Jacoby, P. C.; Pelisser, F. Pozzolanic effect of porcelain polishing residue in Portland cement. *Journal of Cleaner Production*, v. 100, p. 84- 88, 2015.
- [21] KUMMER, L. et al Reutilização dos resíduos de polimento de porcelanato e feldspato na fabricação de novos produtos cerâmicos. *Cerâmica Industrial*, v. 12, n. 3, p. 34-38, 2007.
- [22] Maciel, M. H. et al. Efeito da variação do consumo de cimento em argamassas de revestimento produzidas com base nos conceitos de mobilidade e empacotamento de partículas. *Ambiente Construído*, Porto Alegre, v. 18, n. 1, p. 245-259, jan./mar. 2018.
- [23] Martins, B. H. R. et al Influência da adição de diferentes finos em argamassa autoadensável. In: Congresso Brasileiro De Concreto, 61., Fortaleza, 2019. Anais [...] Fortaleza, 2019.
- [24] Martins, E. J. Procedimento para dosagem de pastas para argamassa autonivelante Curitiba, 2009. Dissertação (Mestrado em Engenharia Civil) - Escola de Engenharia, Universidade Federal do Paraná, Curitiba, 2009.
- [25] Matos, P. R. Estudo do uso de residuo de polimento e porcelanato em concreto autoadensável Florianópolis, 2019. Tese (Doutorado em Engenharia Civil) - Escola de Engenharia, Universidade Federal de Santa Catarina. Florianópolis, 2019.
- [26] Matos, P. R. et al. Rheological behavior of Portland cement pastes and self-compacting concretes containing porcelain polishing residue. *Construction and Building Materials*, v. 175, p. 508-518, 2018.
- [27] Mattana, A.; Costa, M. Estudo da influência de aditivo dispersante no comportamento reológico de argamassas de revestimento, In: Congresso Português De Argamassas De Construção, 3., Lisboa, 2010. Anais [...] Lisboa, 2010.
- [28] Nakakura, E. H.; Bucher, H. R. E. Pisos autonivelantes: propriedades e instalações. In: Simpósio Brasileiro De Tecnologia Das Argamassas, 2., Salvador, 1997. Anais [...] Salvador, 1997.
- [29] Oliveira, I. R. et al Dispersão e empacotamento de partículas São Paulo: Fazendo Arte, 2000.
- [30] Pelisser, F.; Steiner, L. R.; Bernardin, A. N. Recycling of porcelain tile polishing residue in Portland cement: hydration efficiency. *Environmental Science & Technology*, v. 46, n. 4, p. 2368-2374, 2012.
- [31] Romano, R. C. O. et al. Viscosidade cinemática de pastas cimentícias com incorporadores de ar avaliadas em diferentes temperaturas. *Cerâmica*, v. 58, p. 58-65, 2012.

[32] Romano, R. C. O. et al Avaliação do estado endurecido de argamassas de revestimento em função da variação do consumo de cimento. In: Simpósio De Argamassas e Soluções Térmicas De Revestimento, 2., Coimbra, 2016. Anais [...] Coimbra, 2016.

[33] Silva, G. J. B. Estudo do comportamento do concreto de cimento Portland produzido com a adição do resíduo de polimento do porcelanato Belo Horizonte, 2005. Dissertação (Engenharia Metalúrgica e de Minas) - Escola de Engenharia, Universidade Federal de Minas Gerais, Belo Horizonte, 2005.

[34] Souza, P. A. B. F. Estudo do comportamento plástico, mecânico, microestrutural e térmico do concreto produzido com o resíduo do porcelanato 2007. Tese (Doutorado em Ciência e Engenharia de Materiais) - Escola de Engenharia, Universidade Federal do Rio Grande do Norte, Natal, 2007.

[35] Souza, C. H. B. Desenvolvimento de argamassas de revestimento com adição do resíduo do polimento do porcelanato Recife, 2013. Monografia (Trabalho de Conclusão de Curso) - Universidade Federal de Pernambuco, Recife, 2013.

[36] Steiner, L. R. Efeito do rejeito de polimento do porcelanato na fabricação de blocos de concreto de cimento Portland Criciúma, 2011. Monografia (Especialização em Engenharia Civil) - Pós-Graduação em Engenharia Civil, Universidade do Extremo Sul de Santa Catarina, Criciúma, 2011.

[37] Steiner, L. R.; Bernardin, A.; Pelisser, F. Effectiveness of ceramic tile polishing residues as supplementary cementitious materials for cement mortars. *Sustainable Materials and Technologies*, v. 4, p. 30-35, 2015.

[38] Steiner, L. R. Efeito do resíduo de polimento de porcelanato como material cimentício suplementar Criciúma, 2014. Dissertação (Mestrado em Engenharia Civil) - Universidade do Extremo Sul Catarinense, Criciúma, 2014.

[39] Torres, D. R.; Romano, R. C. O.; Pileggi, R. G. Influência da variação da velocidade de rotação e do tipo de cimento nas propriedades de argamassas de revestimento nos estados fresco e endurecido. *Cerâmica*, v. 63, p. 508-516, 2017.

[40] Uysal, M; Yilmaz, K. Effect of mineral admixtures on properties of self-compacting concrete. *Cement and Concrete Composites*, v. 33, p. 771-776, 2011.